Simple Spec-Based Modelling of Lithium-Ion Batteries

Fiodar Kazhamiaka[1], Srinivasan Keshav[1], Catherine Rosenberg[2], and Karl-Heinz Pettinger[3]

***Abstract*—Lithium-ion battery models that estimate their energy content after a series of charge and discharge operations are essential in the optimal design, analysis and operation of battery-based systems. We focus on the class of battery models that can be calibrated entirely from the battery's manufacturer-provided specifications (spec). Such models are simple to calibrate and are therefore widely used in practice. The best-known model in this category was proposed by Tremblay *et al.* in 2007. This model, however, has several shortcomings, including low fidelity at high C-rates, and the fact that it does not model the battery management system. We propose an alternative, called the Power-based Integrated (PI) model that is also completely spec-based, yet has much higher fidelity. We perform two types of validation, the first one uses the voltage profiles in the spec while the other is based on laboratory experiments. Both validations confirm that our model, which we have publicly released as a Simulink system block, has a mean absolute voltage error of less than 0.1 V across a wide range of C-rates.**

***Index Terms*—Lithium-ion battery, Storage, Modeling, Simulink**

I. Introduction

Lithium-ion batteries lie at the heart of many modern devices and systems, including smartphones, electric vehicles, and grid-scale energy storage. Models of Lithium-ion batteries, that estimate their energy content after a series of charge and discharge operations, hence play a central role in the optimal design, analysis, and operation of these battery-based systems.

Many battery models have been developed in the past, with varying degrees of computational complexity, ease of use, and fidelity [1]. Some models aim to simulate the electro-chemical processes within a battery, or emulate battery behaviour using electrical circuits; these approaches have been shown to be highly accurate, but are computationally complex and therefore not suitable for use in optimization or large-scale simulation studies. Other models are based on neural networks, which model the battery directly [2] or are used to tune model parameters ([3], [4]).

Calibrating the parameters for these modelling approaches is a challenge. For example, circuit-based models require pulse-current charge/discharge voltage measurements from which model parameters are extracted ([5], [6], [7], [8], [9], [10], [11], [12]), while neural network approaches require data sets of battery measurements for training the network. These data sets are difficult to obtain, making the models challenging to use in practice.

In contrast, some models can be calibrated using only the information typically found in the specifications document (spec sheet) released by a manufacturer of the battery cells[1]. A spec sheet typically includes information about nominal capacity, internal resistance, and voltage vs. ampere-hour curves for battery charging and discharging at different currents. Thiruganam *et al.* [13] propose a model that can be calibrated using only the information found in the spec sheets released by battery manufacturers like EIG, Sony, Panasonic, and Sanyo. Their parameter calibration approach is complex, involving the use of a genetic algorithm to fit the polynomial function parameters of their model to the voltage curves from a spec sheet. A simpler and more widely used *spec-based* model, i.e., model parameters are computed using only the spec, for simulation[2] was proposed by Tremblay *et al* [15] for four different battery chemistries: Lithium-ion, Lead-acid Nickel-Cadmium, and Nickel-Metal-hydride. A later publication [16] describes improvements to the model equations that are specific to each battery chemistry, and presents experiments that are used to evaluate the accuracy of the models.

One of the defining features of the model proposed in [16] by Tremblay *et al.* for Lithium-ion batteries (that we refer to as the *TD* model) is how easy it is to obtain the model's parameter values, which can be extracted from the spec sheet and used directly in the model without any additional work. Specifically, the parameters can be calculated using the internal resistance (Ohms), nominal capacity (Ampere-hour), the voltage at full charge (Volts), and two points on a nominal voltage curve (Ampere-hour, Volts) at a particular C-rate. This simplicity is a major reason for the widespread use of the TD model for simulating battery systems over more advanced models[3].

Despite its widespread use, the TD model has some shortcomings:

1) **The input to the model is current**. When conducting a power flow simulation of a power system that includes a battery, it is desirable to have a battery model that uses power as input because power is conserved, whereas current may go through many transformations, which would have to be explicitly modeled if the battery model expects current as input.

F. Kazhamiaka and Prof. S. Keshav are with the Cheriton School of Computer Science [1], and Prof. C. Rosenberg is with the Electrical and Computer Engineering Department [2] at the University of Waterloo, 200 University Ave. West, Waterloo, Ontario, Canada. fkazhami at uwaterloo.ca, keshav at uwaterloo.ca, cath at uwaterloo.ca

K.-H. Pettinger is a Professor of Electrical Energy Storage with the Faculty of Mechanical Engineering at Landshut University of Applied Sciences [3], Am Lurzenhof 1, Landshut, Germany. karl-heinz.pettinger at haw-landshut.de

[1]Examples of spec sheets can be found at http://category.alldatasheet.com

[2]We discuss other widely-used models, developed for the goal of system optimization, in [14]

[3]Google Scholar indicates over 500 citations to each of [16] and [15].

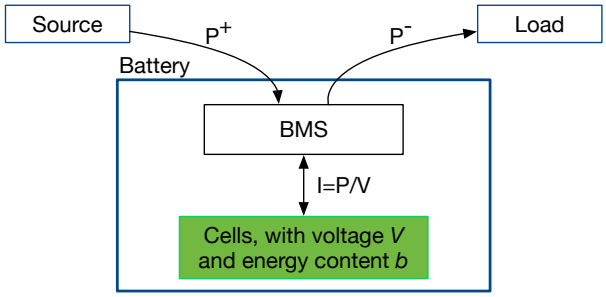

Fig. 1. The battery system.

2) **The battery management system (BMS) is not modelled**. A battery has two components: the cells, each one being an electrochemical system that can store energy, and the BMS, which protects the cells from being damaged due to improper use such as under/over-charging. The TD model characterizes the behaviour of a cell but not the BMS, fuses, and wiring, and therefore allows the simulated battery to be used in a way that would be prevented by a BMS.
3) **The model is not accurate over a wide range of charging and discharging rates**. In the evaluation of the TD model for Lithium-ion batteries [16], the experiments were conducted using a limited range of charging and discharging rates. A more thorough evaluation over a larger range of currents and full charge-discharge cycles (presented in this paper) shows that the model's accuracy is poor for some charging and discharging rates depending on the Lithium-ion technology.

In this paper, we present the Power-based Integrated (PI) Lithium-ion battery model which can be used for simulation studies of energy system design, operation, and analysis involving such a battery. This model is easy to calibrate from a standard spec sheet and uses power as input, rather than current. It also models the functionality of a BMS. We perform two types of validation, the first one uses the voltage profiles in the spec as a benchmark, while the other is based on laboratory experiments. We perform the validation for two different Lithium-ion battery chemistries and find that the PI model is significantly more accurate than the TD model. Our model is freely available in the public domain as a Matlab system block compatible with Simulink simulation software.

The rest of this paper is organized as follows. Section II describes the model formulation and assumptions. Section III describes the parameter calibration. Our model is validated against spec voltage curves in Section IV, and with additional experiments in Section V. We describe our Matlab system block implementation in Section VI.

II. Power-based Integrated (PI) Model

Fig. 1 shows the system under study. The battery is composed of a BMS and Lithium-ion cells. The BMS protects the cells from damage, preventing the battery from being charged or discharged at too high a power, or for the battery's voltage to lie outside a pre-defined range. Given this system, we model the change in the battery system's energy content due to charging or discharging at a particular power level.

Specifically, let $P(k)$ denote the charge/discharge power (in Watts) during time step k. $P(k)$ is positive if the battery is being charged and negative if it is being discharged. The length of each time step is denoted T_u (measured in seconds); in our work T_u is typically between one and 300 seconds. Some battery parameters depend on the current and voltage, which are not inputs, so the model use the power $P(k)$ to compute internal estimates of the current, denoted $I(k)(P(k))$ or, in short $I(k)$ (in Amperes), and terminal voltage $V(k)(P(k))$, or, in short, $V(k)$ (in Volts).

Our model answers three questions:

Q1: Is $P(k)$ infeasible, because the charge/discharge power exceeds the battery's power limits, or will cause the battery voltage to go beyond the recommended range?
Q2: If not feasible, what is the highest feasible power that can be applied?
Q3: If feasible, what is the new state of the battery?

Q1 and Q2 are related to the BMS functionality, and Q3 relates to the evolution of the battery energy content over time.

Hence, given the battery system parameters (defined later) and the battery energy content at time $k-1$, denoted $b(k-1)$, the outputs of the model (when $P(k)$ is feasible) are the energy content of the battery $b(k)$ (in Watt-hours) and the two internal variables of our model, i.e., the current $I(k)$ and voltage $V(k)$, at the end of time slot k.

We refer to our model as the Power-based Integrated model (PI model for short), since it integrates the functions of a BMS and uses power as input. The model uses the applied power and initial energy content to jointly compute the energy content, applied current, and voltage, making use of a spec-derived function which maps energy and current to voltage.

A. Description and Formulation

Lithium-ion batteries are complex electrochemical systems and a typical spec sheet does not capture all aspects of battery behaviour. To account for this, we make the following modeling assumptions. First, we assume that the battery temperature, its internal resistance and its state of health[4] do not change over the course of operation of the model. Second, we assume that the voltage memory effect [17] can be ignored. The implications of these assumptions are discussed in Section VII.

We now describe our model in more detail. The PI model incorporates the following high-level characteristics of Lithium-ion batteries:

- **Charging and discharging penalties** We model battery charging and discharging inefficiences as penalty functions of the current and voltage $\eta_c(I,V)$ and $\eta_d(I,V)$. $\eta_c(.)$ represents the fraction of applied power that is stored in the battery when it is being charged at power P, i.e., $(1-\eta_c(.))P$ is the power loss penalty due to charging inefficiency. Symmetrically, $\eta_d(.)$ represents the power that needs to be discharged in order to obtain

[4]Spec sheets are mostly representative of new batteries; if the state of health degrades then model parameters will need to be adjusted.

power $P < 0$ from it, i.e., the battery loses energy at a rate $\eta_d(.)P$. Note that $\eta_c(.) \leq 1$ and $\eta_d(.) \geq 1$.

- **Charging/discharging rate limits** To avoid overheating, the BMS ensures that the battery cannot be charged or discharged too quickly. In our model, α_c denotes the maximum charging current, and α_d the maximum discharging current.
- **Energy content limits** A BMS limits the battery voltage to the range $[V_{min}, V_{max}]$ to prevent the rapid degradation of its state of health. The amount of energy that can be obtained from a battery that is initially fully charged before the voltage reaches V_{min} depends on the discharging current being applied [18]. Similarly, the charging current affects the amount of energy that can be stored in the battery before the voltage reaches V_{max}. In our model, instead of a permissible *voltage* range, we specify a permissible *energy content* range, using content limits that are functions of the current (which in turn depends on the charge/discharge power $P(k)$). Specifically, the upper limit $a_1(I)$ is the energy content at the point when the voltage reaches V_{min} while being discharged with a current of I and the lower limit $a_2(I)$ is the energy content at the point when the voltage reaches V_{max} when being charged at a current I.

The following set of equations and constraints describes the PI model:

$$b(k) = b(k-1) + \Delta_E(k) \quad (1)$$

$$\Delta_E(k) = \begin{cases} \eta_c(I(k), V(k))P(k)T_u & : P(k) \geq 0 \\ \eta_d(I(k), V(k))P(k)T_u & : P(k) < 0 \end{cases} \quad (2)$$

$$V(k) = M(b(k), I(k)) \quad (3)$$

$$I(k) = \frac{P(k)}{V(k)} \quad (4)$$

$$\alpha_d \leq I(k) \leq \alpha_c \quad (5)$$

$$a_1(I(k)) \leq b(k) \leq a_2(I(k)) \quad (6)$$

Eqs. (1) and (2) indicate that the energy content at the end of time slot k is simply the energy content at the end of time slot $k-1$ plus (resp. minus) the energy put into (resp. drawn from) the battery in time slot k due to charging (resp. discharging). Eq. (3) maps the energy content and the charge/discharge current to the battery voltage, and will be discussed at length in the next subsection. The two internal variables $I(k)$ and $V(k)$ are *also* related through Eq. (4) which states that the power is the product of current and voltage. Eqs. (5) and (6) have been discussed above.

The PI model is therefore characterized by two parameters (α_c, α_d), and the five functions $\eta_c(I, V)$, $\eta_d(I, V)$, $a_1(I)$, $a_2(I)$ and $M(b, I)$. Given the energy content of the previous time slot $b(k-1)$ and a feasible input power $P(k)$, the model calculates the battery energy content $b(k)$, voltage $V(k)$, and current $I(k)$. In the next subsections, we will discuss Eq. (3) and how to use it. Section III explains how to calibrate these parameters and functions using the battery's spec sheet.

B. The function M

Most battery spec sheets provide a family of curves that represent the battery's terminal voltage as a function of its

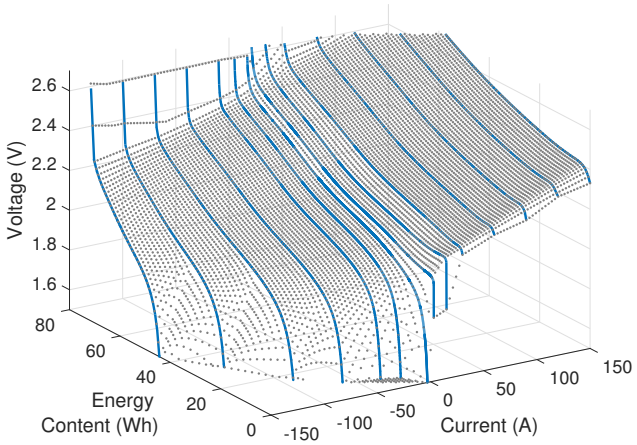

Fig. 2. M function, showing the terminal voltage as a function of energy content and charge/discharge current. The blue lines are the reversible capacity curves measured for a Li-Titanate cell [19]. The function, in grey, is a discretization of the underlying continuous surface.

'reversible capacity[5]' when discharging or charging a cell at different rates. Fig. 4 and Fig. 5 (reproduced from [19]) show these functions for the Leclanché Li-Titanate cell. Although the spec sheet only provides this data for some C-rates, we can view these curves as representing a continuous surface. A key insight in our work is to use a *mesh* function M (a discretization of the underlying continuous surface) to map the battery energy content and charge/discharge current to the battery's voltage. This function, which can be derived from the spec sheet's reversible capacity voltage curves (see Fig. 4 and Fig. 5), captures the inherent non-linearities in battery voltage behaviour. An example can be seen in Fig. 2. Intuitively, M represents all feasible combinations of energy content, charge/discharge current, and battery voltage.

We now discuss how to use the M function to compute the change in battery voltage due to a certain amount of power injection or discharge $P(k)$. Note that the battery voltage has to be feasible (lie on the surface discretized by M) and consistent with the amount of power injected/discharged, i.e., $V(k) = P(k)/I(k)$. If M had been defined in the space $< I(k), P(k), V(k) >$, this would correspond to finding the intersection, if it existed, between the curve $V(k)I(k) = P(k)$ and the surface described by M. However, M is defined in the space $< I(k), b(k), V(k) >$ not $< I(k), P(k), V(k)$. Thus, we need to define an auxiliary space, as discussed next.

Consider the subset of the M surface that is described by:

$$\begin{aligned} S := \{< I, b, V >: \ & \alpha_d \leq I \leq \alpha_c, \\ & a_1(I) \leq b = b(k)^I \leq a_2(I), \\ & V_{min} \leq V = M(b, I) \leq V_{max}\}, \end{aligned}$$

where $b(k)^I$ is calculated using I as the estimate for current using Eqs. (1) and (2). By construction, every point in S satisfies all of the constraints of the model except for Eq. 4, i.e., $P(k) = V(k)I(k)$.

[5]This term is explained in Section III-B.

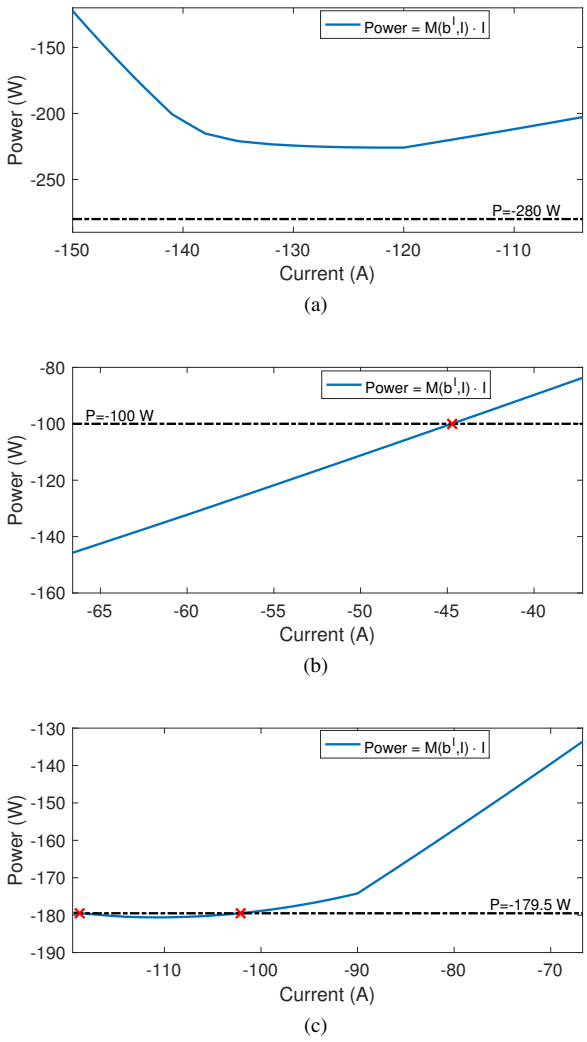

Fig. 3. Three cases: No intersection (a), one intersection (b), and multiple intersections (c). A red cross indicates an intersection.

We then construct, in an auxiliary 2D space $< I, P >$, the line $y = P(k)$ (this is the given power injection/discharge) and the curve $y = VI$ for all points $(I, b, V) \in S$. The latter curve is obtained by enumerating all points in S, then computing, for each point, the corresponding pair of $(I, V.I)$. The next step is to compute the intersection(s), if any, between these two curves. We do so by examining the points on the curve $y = VI$ (in increasing order of I) looking for adjacent pairs of points $< I_1, V_1 >$and $< I_2, V_2 >$ such that the sign of $P - V_1 * I_1$ is different from that of $P - V_2 * I_2$. The difference in sign indicates an intersection in between the two points, in which case we linearly interpolate between the points to get an estimate for the value of I at the point of intersection. b and V values are then computed using this estimate.

Now, there are three possible cases (an example for each case is shown in Fig. 3):

a) No intersection: There are no *feasible* voltage and current estimates for the given $P(k)$ and $b(k-1)$ (see Fig. 3(a)). In that case, the power is iteratively reduced by a small quantum value and S is recomputed for each value of $P(k)$ until an intersection is found. This value of $P(k)$ is the maximum feasible power that the BMS can allow.

b) One intersection: Let that intersection point be $(I^*, P(k))$ (see Fig. 3(b)). In that case, I^* is the estimate for $I(k)$ and $V(k) = \frac{P(k)}{I^*}$ the voltage estimate.

c) Multiple intersections: The non-linearity of the surface makes it possible for multiple intersections to occur, as shown in Fig. 3(c). This case happens rarely for the Lithium-ion cell chemistries we have tested, and only occurred near the steep part of the voltage curve[6]. There are many potential approaches to choosing one of the multiple intersection points as our estimate. To preserve the continuity of voltage estimates over time, we recommend choosing the point yielding a voltage estimate which is the closest to the voltage value estimated for the preceding time step ($V(k-1)$).

Next, we explain how to calibrate our model.

TABLE I
BATTERY SPECIFICATIONS

Value	Li-Titanate	$LiFePO_4$
Nominal Capacity (Ah)	30	1.1
V_{min} (V)	1.7	2
V_{max} (V)	2.7	3.6
Internal Impedance (ω)	0.002	0.05
Max. charge (discharge) C-rate	4 (4)	4 (10)

III. Model Calibration

Calibrating the parameters of the model requires a battery spec sheet. We use the Leclanché Li-Titanate cell specifications document [19] as an example. Note that although the description of our model calibration process may appear complex, its inputs are easily obtained and the calculations are relatively simple. For example, although we present some equations as integrals, in practice we compute these numerically as a Riemann sum. Moreover, this calibration process has been automated as part of our Simulink implementation.

In a typical spec sheet, charging and discharging currents are expressed in terms of a *C-rate*, where 1C is defined as the current needed to fully charge or discharge the nominal capacity of the battery (which is specified in the spec sheet) in 1 hour. For the Li-Titanate cell, 1 C corresponds to a 30A, because the nominal capacity is 30Ah. Table I shows the spec data (excluding voltage curves) for the Li-Titanate and $LiFePO_4$ cells.

A. Charge/discharge penalty functions: $\eta_c(I,V), \eta_d(I,V)$

Let R_{ic} and R_{id} denote the internal impedance values (provided by the spec) during charging and discharging, respectively. Note that some specs provide only a single value R_i for internal impedance; in that case, $R_{ic} = R_{id} = R_i$. Then, it is easy to show that:

$$\eta_c(I,V) = 1 - \frac{IR_{ic}}{V} \text{ for } I > 0 \quad (7)$$

$$\eta_d(I,V) = 1 - \frac{IR_{id}}{V} \text{ for } I < 0 \quad (8)$$

[6]The steep part of the voltage curve is seldom visited by many applications because of the practice of restricting the state of charge to preserve battery lifetime [20].

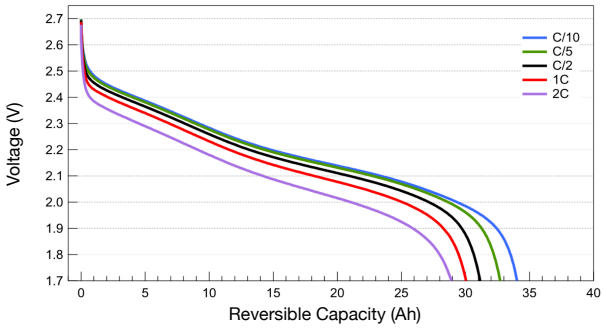

Fig. 4. Voltage vs. charge content for different discharge rates [19].

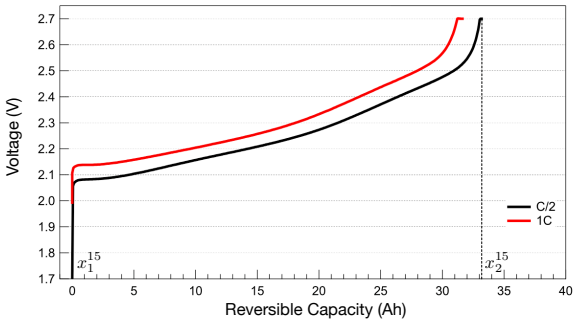

Fig. 5. Voltage vs. charge content for different charge rates [19]. x_1 and x_2 for a C/2 charging current (15 Amperes) are labeled.

B. Voltage function: M

We now discuss how to calibrate the M function. Recall that battery spec sheets provide the terminal voltage as a function of 'reversible capacity' when discharging or charging a cell at different C-rates. 'Reversible capacity,' expressed in units of Ah or Coulombs, is the amount of charge added or removed from the battery. Since the curve is expressed in volts, and 1 Joule = 1 Volt-Coulomb = 1 Watt-second, the area under each curve in Fig. 4 indicates how much energy can be discharged from the battery at the given C-rate. It is clear that as the C-rate increases, the energy capacity of the battery decreases. Similarly, the area under each curve in Fig. 5 represents the energy needed to charge an empty battery at given C-rate.

Let x_1^I and x_2^I be the initial and final charge content of the battery that is being charged or discharged at current I, i.e., when the voltage reaches V_{min} or V_{max} respectively. For example, the x_1^I and x_2^I values have been labeled in Fig. 5 for the C/2 curve ($I = 15$ Amperes). Correspondingly, let $V^I(x)$ be the voltage when the battery charge content is x while current I is applied. Let $E_d^I(Q)$ be the energy drawn from a full battery when Q Coulombs are discharged at current I, and $E_c^I(Q)$ be the energy content of the battery when it is charged to Q Coulombs using current I. Finally, let $V^I(Q)$ be the battery voltage when current I is applied and the battery reversible capacity is Q Coulombs. Then,

$$E_d^I(Q) = \int_{x_1^I}^{Q} V^I(x)\eta_d(I,V)\ dx \tag{9}$$

$$E_c^I(Q) = \int_{x_1^I}^{Q} V^I(x)\eta_c(I,V)\ dx, \tag{10}$$

and each point in the M function can be calculated as:

$$M(I, E_d^I(Q)) = V^I(Q) \text{ for } I < 0 \tag{11}$$

$$M(I, E_c^I(Q)) = V^I(Q) \text{ for } I > 0. \tag{12}$$

In practice, we numerically evaluate the integral as a Riemann sum, where the $(x, V^I(x))$ tuples are obtained by digitizing the curves from the spec sheet using a standard plot digitizer[7] and linearly interpolating between the C-rate curves using a suitably fine digitization grid. Fig. 2 shows the M mesh for the example Li-Titanate cell. This maps the energy content in the domain [0 Wh,72.5 Wh] and current in the domain [-5 C, 5 C] to a voltage in the range [1.5 V, 2.7 V].

C. Energy Content Limits: $a_1(I), a_2(I)$

The upper and lower limits on energy content can also be derived from the voltage vs. reversible capacity curves in the spec sheet. By definition, $a_1(I)$ is the energy remaining in a battery when the voltage reaches V_{min} while being discharged with current I, i.e., $a_1(I) = E_d^{max} - E_d^I(x_2^I)$, where E_d^{max} is the maximum[8] $E_d^I(x_2^I)$ over all I. Similarly,$a_2(I)$ is the energy in the battery when the voltage reaches V_{max} at current I, i.e., $a_2(I) = E_c^I(x_2^I)$. Summarizing:

$$a_1(I) = E_d^{max} - E_d^I(x_2^I) \tag{13}$$

$$a_2(I) = E_c^I(x_2^I) \tag{14}$$

D. Charging/Discharging limits: α_c, α_d

The spec sheet almost always gives recommended maximum charging and discharging C-rates, which are used directly. α_c is the maximum charge current, and α_d is the maximum (negative) discharge current.

IV. Validation Against Spec

In this section, we evaluate the ability of our model to reproduce the voltage curves found in the spec. We simulate constant current charging and discharging on the PI model, using the same charging rates that were used to obtain the voltage curves from the spec and evaluate how closely the spec voltage curves are reproduced.

We compare the PI model against two versions of the TD model. The first version is the default implementation of the model in Simulink. Since the default TD model does not include a BMS, we created a second version of the model (referred to as the TDB model) that incorporates a BMS which keeps the cell voltage at the voltage limit when the TD model's

[7] We use the online tool available at https://automeris.io/WebPlotDigitizer/

[8] Typically, the maximum amount of energy is obtained by using a very low discharging current

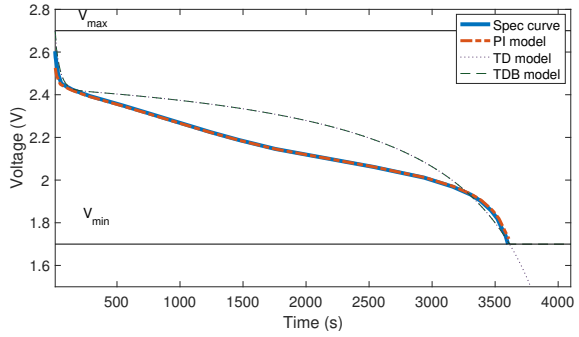

Fig. 6. Li-Titanate cell discharged at 1C.

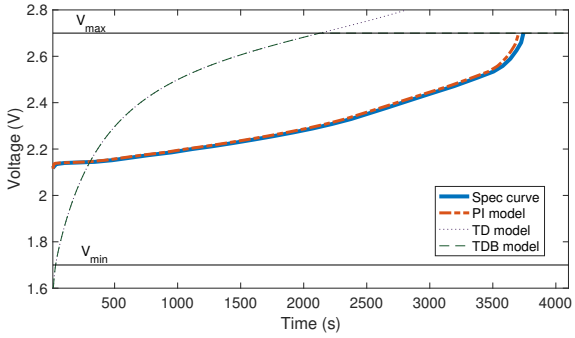

Fig. 7. Li-Titanate cell charged at 1 C constant current.

voltage would otherwise exceed the limit. This allows a fairer comparison of the TD and PI models. The simulation files and the experimental data used to evaluate our model are freely available on Github[9]. Note that although the model presented by Thirugnanam *et al* in [13] can also be calibrated using a spec, doing so requires extensive additional work in setting up the genetic algorithm optimizer to obtain the model parameters and is hence more difficult to use than the PI and TD/TDB models. Hence, we compare our PI model with real voltage curves, as well as the TD and TDB models.

We calibrate the PI model using all the voltage curves in the spec of the Li-Titanate and $LiFePO_4$ cells; the TD and TDB models use the 1 C Li-Titanate discharge voltage curve and the 4.55 C $LiFePO_4$ discharge voltage curve[10] from the spec. Note that the Li-Titanate cell spec has voltage curves for up to 2 C discharging and 1 C charging and the $LiFePO_4$ spec has curves for up to 9.1 C discharging and no charging voltage curves.

Fig. 6 compares the models against the 1 C discharging curve from the Li-Titanate spec. The PI model replicates this curve very well, unlike the TD and TDB models. A similar pattern is seen in Fig. 7 for the Li-Titanate cell charged at 1 C. For the $LiFePO_4$ technology, Fig. 8 compares model performance for a 4.55 C discharging curve. All models replicate the curve well for this technology, although the TD model has higher errors at the start of the discharge.

[9] https://github.com/iss4e/PIModel_Testing.git

[10] The voltage curve with the lowest current in the $LiFePO_4$ spec sheet was measured at 5 A, which is 4.55 C.

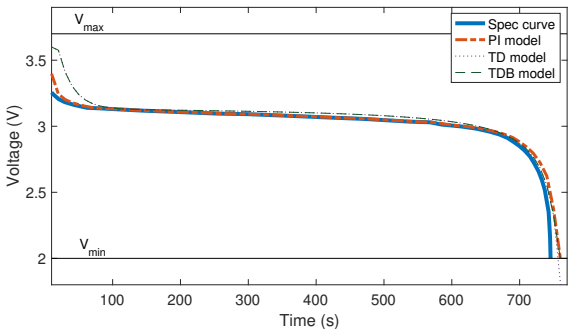

Fig. 8. $LiFePO_4$ cell discharged at 4.55 C constant current.

Fig. 9 shows the MAVE for Li-Titanate spec voltage curves. The PI model has very low error on average, especially compared to the TD and TDB models. The same comparison for $LiFePO_4$ cells is given in Table II, since there are only two voltage curves to compare against in the spec of this cell. TD and TDB models behave similarly because the BMS is rarely active during these tests.

V. Further Validation with Experimentation

The spec sheets for the cells used in our evaluation include reversible capacity curves for a limited number of charging and discharging currents. Furthermore, the spec sheet characterizes an average cell, but each individual cell may vary slightly due to the manufacturing process. To better evaluate our model, we measured voltage curves over a wider range of charging and discharging currents using the setup described in Section V-A for several cells described below. For example, the spec sheet for the Li-Titanate cell shows voltage curves for currents up to 2 C, but recommends a maximum charging current of 4 C; to increase the scope of our evaluation, we ran experiments to obtain voltage curves for discharging rates all the way up to 5 C to test beyond the limits of the spec sheet. We use measured voltage curves for parameter calibration of all the models being evaluated to avoid introducing errors that are caused by inconsistencies between the voltage curves of the cells in our experiments and their corresponding spec. Specifically, the PI model is parameterized using measured voltage curves across the full range of C-rates measured in our experiments, while the TD and TDB models use the 1 C discharging curve for both Li-Titanate and $LiFePO_4$ cell tests. Section V-B describes the constant-current testing that goes all the way to 4 C charging and discharging recommended by the spec, as well as 5 C where the voltage curve is more non-linear and hence more difficult to model. Section V-C covers the validation on a 'real-world' power profile.

A. Experimental Setup

We performed a series of experiments on two Li-Titanate and two $LiFePO_4$ energy storage cells under different conditions. Each experiment consists of a single-cell battery that is charged or discharged according to an experiment profile.

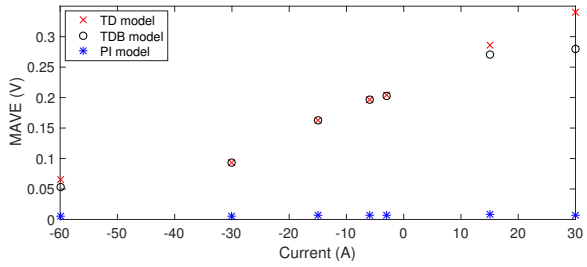

Fig. 9. MAVE for Li-Titanate spec voltage curves.

(a) (b)

Fig. 10. Experimental setup. (a) Li-Titanate cell in temperature chamber (a), and (b) two $LiFePO_4$ cells connected to the power brackets.

TABLE II
MAVE FOR $LiFePO_4$ SPEC VOLTAGE CURVES

C-rate	PI	TD	TDB
-9.1	0.012	0.039	0.039
-4.55	0.011	0.12	0.12

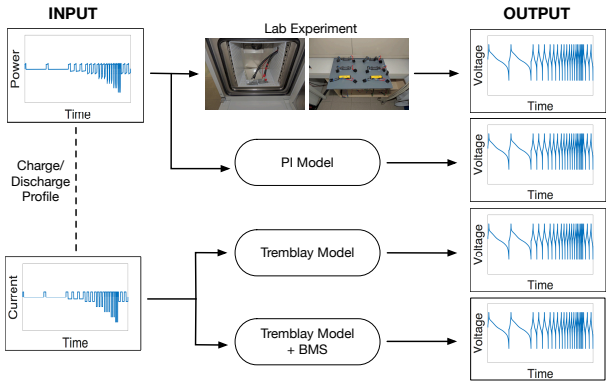

Fig. 11. Evaluation setup. Charge/discharge profiles were tested on real cells, our PI model, and two implementations of the TD model.

The Li-Titanate cells [19] have a voltage range of [1.7[11],2.7] V, and nominal capacity of 30 Ah, although with low discharging rates a capacity of at least 32.7 Ah is possible. The $LiFePO_4$ cells [21] have a voltage range of [2.0,3.6] V, and nominal capacity of 1.1 Ah.

The experiments were conducted using BaSyTec XCTS Lab battery testing equipment (manufactured by BaSyTec GmbH, Germany), which has a programmable interface for specifying the charging and discharging processes of a cell, and hence can mimic a BMS programmed to prevent the battery voltage from going beyond $[V_{min}, V_{max}]$. The cells were connected using a 4-wire connection to the test machine. The equipment gives precise measurements of battery voltage and current. The cells were placed in a Binder MK 53-E2 temperature control chamber (Binder GmbH, Germany) to keep the ambient temperature at a constant 21 degrees Celsius during testing. Fig. 10 shows the lab testing environment.

Most of the experiments involve charge/discharge cycling of the cell under different currents and recording the current, voltage, and total charge (Ah) every 10 seconds. We also ran experiments using a variable charge/discharge profile that reflects how a battery would be used to provide energy storage for a system with a solar power source and building load over an 8-hour period, with a measurement granularity of 1 second. To create this profile, we took 8 hours of solar PV power generation and building load data measured on-site at the Technology Center for Energy at University of Applied Sciences Landshut, Germany, and used it to construct the charge/discharge pattern of a battery if it were used to buffer the excess solar energy and serve the building load. Fig. 11 offers a visualization of how the PI, TD, and TDB models were run on the same charge/discharge profile as the real cells in our experiments, with the measured voltage used as the benchmark.

B. *Constant-current tests*

The results from experiments on constant-current charging and discharging at various C-rates are summarized in Fig. 12 for Li-Titanate and Fig. 13 for $LiFePO_4$ cells. The PI model with measured parameters has a MAVE lower than 0.1 V for all C-rates tested, while the TD and TDB models have much higher errors at high C-rates compared to low C-rates.

C. *Real-world profile experiment*

Fig. 14 compares the voltage estimates of PI and TD models with the measured voltage when using a 'real-world' varying charge/discharge profile on a Li-Titanate cell. This test shows the effectiveness of the PI model beyond constant-current testing, and mimics the real-world application of a battery used to balance PV generation with building power consumption. The PI model estimates the voltage with very low errors, with 0.016 V error on average for the PI model with spec parameters and 0.008 V error with measured parameters, especially relative to the errors of the TD model (0.128 V error, on average) under the same conditions. Note that the BMS is not active in this experiment, hence the TD and TDB models give the same voltage estimate.

D. *Discussion*

The large difference in the accuracy of the PI model compared to the TD model can be at least partially explained

[11]In the experiments with the Li-Titanate cell, we allowed the voltage to drop to 1.5 V, which is lower than the recommended minimum of 1.7 V given by the spec.

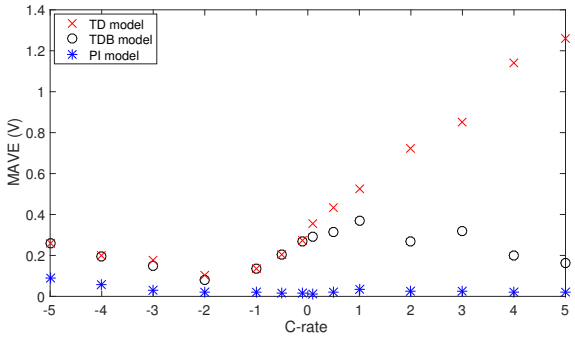

Fig. 12. Li-Titanate MAVE with respect to measured voltage curves.

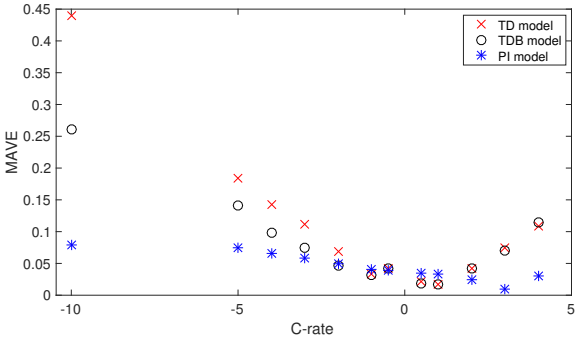

Fig. 13. $LiFePO_4$ MAVE with respect to measured voltage curves.

by noting that the TD model uses only a few points along a single discharging voltage curve for parameter calibration. While this is sufficient to characterize the voltage of the battery at the rate that is used for model calibration for some cell chemistries (as seen in Fig. 8), it is not sufficient for Li-Titanate cells (Fig. 6 and Fig. 7), nor to cover the wide range of charging and discharging rates that can be used by a real application (Figs. 9, 12, 13, and Table II). The PI model makes use of the entire voltage curve across the full range of available charging and discharging rates, and is hence able to model voltage behaviour across the full range, and can accurately model the voltage profiles of different Li-ion chemistries.

VI. Simulink Implementation

The PI model has been implemented as a Matlab system block that is compatible with Simulink simulation software[12]. In addition to implementing the equations of the model, the following user-friendly features have also been included.

- **Automated Parameter Estimation** The parameter estimation has been fully automated. The user specifies the files containing voltage curves as <c-rate, ampere-hour, voltage> tuples which can be extracted from the reversible capacity voltage curves found in the spec sheet using freely available online graph digitizing tools. The user also specifies the nominal capacity, internal impedance, maximum charging and discharging current, initial energy content, and the length of time steps for the discrete simulation.
- **Smart BMS** The constraints on energy content and applied power are implemented so that the model throws a software exception when a constraint is violated. The user can adjust the power according to the information provided by the exception. The exception provides the user with the maximum power that the model could charge/discharge without violating the constraint. This allows the user to implement a 'smart' BMS that makes smooth adjustments to the input power to keep the battery operating safely; we provide an example of how to capture and respond to the exception, along with the model itself, on Matlab File Exchange.
- **Parameter Extrapolation** In cases where the spec sheet fails to provide the voltage curves for the full operating range of the cell, the model uses a linear extrapolation of the available data to obtain the full voltage curve. This is not ideal for model accuracy, but keeps the model usable in the absence of data.

[12]Matlab File Exchange link: https://www.mathworks.com/matlabcentral/fileexchange/63078-lithium-ion-pi-model

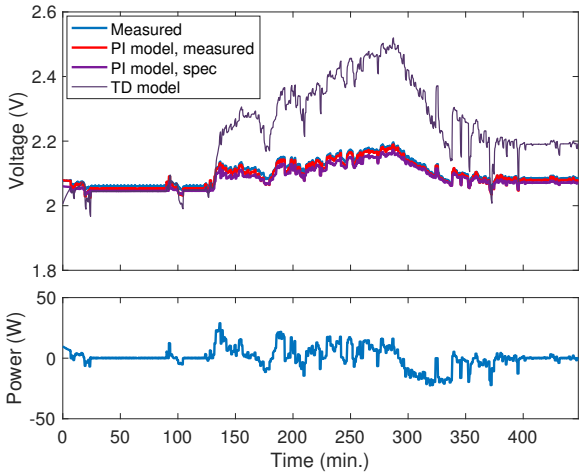

Fig. 14. Li-Titanate battery voltage for the given charge/discharge profile.

VII. Limitations and Conclusion

In contrast to the widely-used spec-based Lithium-ion battery model proposed by Tremblay *et al*, we propose the Power-based Integrated (PI) model. The PI model is similar to the TD model in terms of the effort required to calibrate the model parameters. However, it has a higher fidelity across a wider range of charge/discharge currents. Moreover, by using power as input, rather than current, it makes the overall system model easier to build, and by modeling the functionality of a Battery Management System it is more complete. The PI model has been validated for two different battery chemistries and we find that the mean absolute voltage error is consistently below 0.1 V. We have implemented and publicly released the PI model as a Matlab/Simulink system block model.

Our model has two main limitations. It is spec-based and we assume that the following information is present in the spec: voltage curves, nominal capacity and the internal

resistance. Although it is typical for at least a few voltage curves and the nominal capacity to be included in the spec, not all spec sheets provide the same information. In cases where only a limited number of voltage curves is provided, the model would interpolate and extrapolate based on the available data. In cases where the internal resistance is not provided, it would have to be obtained through experiments or approximated using information available from the Internet for the given cell chemistry. The second limitation is the problem of multiple feasible combinations of cell voltage and current, as described in Section II-B, which is inherent to discrete power-based models. A given power can suggest multiple feasible combinations of cell voltage and current in rare cases, and model estimates in these conditions may not be accurate.

Our model assumes that temperature and internal resistance are constant. In reality, the ambient temperature may vary and charging/discharging the battery increases the internal temperature and affects the voltage of the battery, while the internal resistance varies with the charge of the battery. These dependencies are not typically described in spec sheets (although temperature-dependent voltage curves are becoming more prevalent), and our model assumptions reflect this.

In future work, we plan to investigate the application of the PI model to different battery technologies, such as Lead-Acid, Sodium-Nickel-Chloride, and Redox-Flow batteries. We believe the model will fit a wide range of batteries whose cell energy capacities range from 10 Wh to 100 kWh.

REFERENCES

[1] A. Seaman, T.-S. Dao, and J. McPhee, "A survey of mathematics-based equivalent-circuit and electrochemical battery models for hybrid and electric vehicle simulation," *Journal of Power Sources*, vol. 256, pp. 410–423, 2014.

[2] A. Eddahech, O. Briat, and J.-M. Vinassa, "Neural networks based model and voltage control for lithium polymer batteries," in *Diagnostics for Electric Machines, Power Electronics & Drives (SDEMPED), 2011 IEEE International Symposium on*, pp. 645–650, IEEE, 2011.

[3] G. Capizzi, F. Bonanno, and G. M. Tina, "Recurrent neural network-based modeling and simulation of lead-acid batteries charge–discharge," *IEEE Transactions on Energy Conversion*, vol. 26, no. 2, pp. 435–443, 2011.

[4] C. Piao, X. Yang, C. Teng, and H. Yang, "An improved model based on artificial neural networks and thevenin model for nickel metal hydride power battery," in *Optics Photonics and Energy Engineering (OPEE), 2010 International Conference on*, vol. 1, pp. 115–118, IEEE, 2010.

[5] M. Chen and G. A. Rincon-Mora, "Accurate electrical battery model capable of predicting runtime and iv performance," *IEEE transactions on energy conversion*, vol. 21, no. 2, pp. 504–511, 2006.

[6] A. Hentunen, T. Lehmuspelto, and J. Suomela, "Time-domain parameter extraction method for thévenin-equivalent circuit battery models," *ieee transactions on energy conversion*, vol. 29, no. 3, pp. 558–566, 2014.

[7] T. Huria, M. Ceraolo, J. Gazzarri, and R. Jackey, "High fidelity electrical model with thermal dependence for characterization and simulation of high power lithium battery cells," in *Electric Vehicle Conference (IEVC), 2012 IEEE International*, pp. 1–8, IEEE, 2012.

[8] R. Jackey, M. Saginaw, P. Sanghvi, J. Gazzarri, T. Huria, and M. Ceraolo, "Battery model parameter estimation using a layered technique: An example using a lithium iron phosphate cell," tech. rep., SAE Technical Paper, 2013.

[9] J. Jang and J. Yoo, "Equivalent circuit evaluation method of lithium polymer battery using bode plot and numerical analysis," *IEEE Transactions on Energy Conversion*, vol. 26, no. 1, pp. 290–298, 2011.

[10] T. Kim and W. Qiao, "A hybrid battery model capable of capturing dynamic circuit characteristics and nonlinear capacity effects," *IEEE Transactions on Energy Conversion*, vol. 26, no. 4, pp. 1172–1180, 2011.

[11] M. Knauff, C. J. Dafis, D. Niebur, H. G. Kwatny, C. Nwankpa, and J. Metzer, "Simulink model for hybrid power system test-bed," in *Electric Ship Technologies Symposium, 2007. ESTS'07. IEEE*, pp. 421–427, IEEE, 2007.

[12] L. W. Yao, J. Aziz, P. Y. Kong, and N. Idris, "Modeling of lithium-ion battery using matlab/simulink," in *Industrial Electronics Society, IECON 2013-39th Annual Conference of the IEEE*, pp. 1729–1734, IEEE, 2013.

[13] K. Thirugnanam, E. R. J. TP, M. Singh, and P. Kumar, "Mathematical modeling of li-ion battery using genetic algorithm approach for v2g applications," *IEEE transactions on Energy conversion*, vol. 29, no. 2, pp. 332–343, 2014.

[14] F. Kazhamiaka, C. Rosenberg, S. Keshav, and K.-H. Pettinger, "Li-ion storage models for energy system optimization: The accuracy-tractability tradeoff," in *Proceedings of the Seventh International Conference on Future Energy Systems*, ACM, 2016.

[15] O. Tremblay, L.-A. Dessaint, and A.-I. Dekkiche, "A generic battery model for the dynamic simulation of hybrid electric vehicles," in *Vehicle Power and Propulsion Conference, 2007. VPPC 2007. IEEE*, pp. 284–289, IEEE, 2007.

[16] O. Tremblay and L.-A. Dessaint, "Experimental validation of a battery dynamic model for ev applications," *World Electric Vehicle Journal*, vol. 3, no. 1, pp. 1–10, 2009.

[17] T. Sasaki, Y. Ukyo, and P. Novák, "Memory effect in a lithium-ion battery," *Nature materials*, vol. 12, no. 6, p. 569, 2013.

[18] N. Omar, P. V. d. Bossche, T. Coosemans, and J. V. Mierlo, "Peukert revisitedcritical appraisal and need for modification for lithium-ion batteries," *Energies*, vol. 6, no. 11, pp. 5625–5641, 2013.

[19] Leclanché, *LecCell 30Ah High Energy*, 02 2014. Lithium-Titanate cell specifications.

[20] A. Millner, "Modeling lithium ion battery degradation in electric vehicles," in *Innovative Technologies for an Efficient and Reliable Electricity Supply (CITRES), 2010 IEEE Conference on*, pp. 349–356, IEEE, 2010.

[21] A123 Systems, *High Power Lithium Ion APR18650M1A*, 2009. LiFePO4 cell specifications.

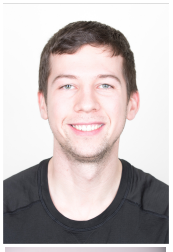

Fiodar Kazhamiaka is a Ph.D. candidate in computer science at the David Cheriton School of Computer Science, University of Waterloo, Waterloo, ON, Canada. His research interests are in the design and control of systems with energy storage and renewable energy sources.

Srinivasan Keshav is a Professor of Computer Science at the University of Waterloo. He received a Ph.D. in Computer Science from the University of California, Berkeley in 1991. He was subsequently an MTS at AT&T Bell Laboratories and an Associate Professor at Cornell. In 1999 he left academia to co-found Ensim Corporation and GreenBorder Technologies Inc. He has been at the University of Waterloo since 2003.

Catherine Rosenberg , FIEEE, is a Professor with the Department of Electrical and Computer Engineering at the University of Waterloo and the Canada Research Chair in the Future Internet. Since April 2018, she is also the Cisco Research Chair in 5G Systems. She was elected a Fellow of the Canadian Academy of Engineering in 2013. Her research interests are in networking, wireless, and energy systems. More information is available at https://ece.uwaterloo.ca/˜cath/.

Karl-Heinz Pettinger is a professor at the Landshut University of Applied Sciences, and is the Scientific Director of the Technology Center for Energy. He is a member of the Advisory Board for Battery Research of the German Ministry of Education and Research, the Lithium Ion Batteries Competence Network and the VDMA Battery Production Group. In his research group, material research, electrode and manufacturing technology development for lithium batteries as well as the integration of lithium storage systems are promoted.